

Pion single charge exchange scattering from ^3He at 285, 428, and 525 MeV

J. Källne,* R. Altemus, P. C. Gugelot, J. S. McCarthy, R. C. Minehart, and L. Orphanos

University of Virginia, Charlottesville, Virginia 22901

P. A. M. Gram, B. Höistad, C. L. Morris, and E. A. Wadlinger

Los Alamos Scientific Laboratory, Los Alamos, New Mexico 87545

C. F. Perdrisat

College of William and Mary, Williamsburg, Virginia 23185

(Received 6 November 1981)

We have measured the cross section of $^3\text{He}(\pi^-, \pi^0)^3\text{H}$ at $T = 285, 428, \text{ and } 525 \text{ MeV}$ for angles in the range of $60^\circ \leq \theta \leq 135^\circ$ covering the momentum transfer range $0.5 \leq q \leq 1.0 \text{ GeV}/c$. Comparison is made with Glauber model calculations to discuss the sensitivity to nuclear structure and pion-nucleus interaction effects.

NUCLEAR REACTIONS $\pi^- + ^3\text{He} \rightarrow ^3\text{H} + \pi^0$, $T = 285, 428, \text{ and } 525 \text{ MeV}$, $\theta_{\pi^0} \approx 70\text{--}140^\circ$; measured $\sigma(\theta_t, T_\pi)$. Analysis based on optical and Glauber model predictions.

In this Communication we present data from the $^3\text{He}(\pi^-, \pi^0)^3\text{H}$ reaction at energies well above the maximum of the 3,3 resonance at angles from 60° to 135° in the center of momentum frame. Single charge exchange (SCE) on free nucleons is related to elastic scattering, but with a rotation in isospin. In this kinematic range, the momentum transfer $q = 2p_\pi \sin\theta/2$ is large ($0.5\text{--}1.0 \text{ GeV}/c$) so that the nuclear structure is sampled in an interesting region of the ^3He form factors. The ^3He nucleus offers a particularly good laboratory for such a study, because its structure is relatively well known from electron scattering. The charge form factor is observed to go through a minimum at $\sim 0.6 \text{ GeV}/c$ (Ref. 1) followed by a broad maximum at $0.7 \text{ GeV}/c$, while the magnetic form factor falls off monotonically out to $0.7 \text{ GeV}/c$, with new measurements indicating a diffraction minimum at $\sim 0.9 \text{ GeV}/c$.² Because of the characteristically different angular dependence of the spin-flip and non-spin-flip parts of the pion-nucleon amplitudes (at the 3,3 resonance, spin-flip varies as $\sin^2\theta_{\text{c.m.}}$, non-spin-flip as $\cos^2\theta_{\text{c.m.}}$), pion scattering can also be used selectively to sample charge and magnetic form factors.

The extraction of nuclear structure information requires knowledge of the pion-nucleus interaction involved in the scattering process as well as theoretical methods to formulate them. Elastic and single charge exchange (SCE) scattering experiments on ^3He and ^4He have provided cross sections with effects attributed to the elementary $\pi + N$ amplitudes and the nuclear structure.³ Some of these features can be interpreted in terms of current theories but are still model dependent and there continue to exist unex-

plained aspects of the data.^{4,5} With regard to the SCE scattering from ^3He , the observed energy dependence between 200 and 300 MeV is not as strong as predicted from existing theories. Early calculations⁶ of the energy variation of the (π^-, π^0) reaction indicated that absorption effects might win out over the $\pi + N$ SCE amplitudes and lead to a flattening of the effective 3,3 resonance. New measurements of $^3\text{He}(\pi^-, \pi^0)$ at 285, 428, and 525 MeV have been made and the information now available for this reaction spans the region 130–525 MeV.

This experiment was performed at the Clinton P. Anderson Meson Physics Facility (LAMPF) using the P^3 pion channel.⁷ The experimental techniques and procedures were similar to those described in Ref. 8. The pion beam intensity was monitored with an ion chamber placed downstream from the target. The target system was a cryostat which maintained liquid ^3He at a temperature of 1.5 K and a thickness of $51 \text{ mg}/\text{cm}^2$. The cryostat windows, heat shields, and Al target cell walls presented a background thickness of $53 \text{ mg}/\text{cm}^2$. The detector consisted of five plastic scintillators ($S1\text{--}S5$) of which $S1\text{--}S3$ provided time-of-flight and differential energy loss information, $S4$ was the stopping counter for particles of interest and $S5$ a veto counter for particles passing $S4$. Particle trajectories and positions were determined with two delay-line wire chambers. The detector subtended a solid angle of 71 msr and 31° in the reaction plane; angles between 25° and 150° were accessible in the laboratory. We could uniquely identify protons, deuterons, and tritons and measure their energies over the ranges $T_p = 22\text{--}150$, $T_d = 34\text{--}205$, and $T_t = 37\text{--}245 \text{ MeV}$. For incident energies of 285,

428, and 525 MeV, we recorded triton spectra for angular bins of about 5° which showed peaks corresponding to the (π^-, π^0) reactions in ${}^3\text{He}$. The counts in this peak minus a background (determined from adjacent portions of the spectrum as shown in Fig. 1) divided by the ion chamber charge gave the relative yield of (π^-, π^0) at each incident energy. Since the negative pion beam has contaminant particles (i.e., e^-, μ^-) at only the few percent level and constant with energy this relative yield is proportional to the cross section. The normalization was obtained by measuring the $\pi^- + p$ elastic scattering yield (detecting the recoil proton) from a CH_2 target at 285, 428, and 525 MeV and comparing to published cross sections.⁹ The uncertainty in the overall scale of the ${}^3\text{He}(\pi^-, \pi^0){}^3\text{H}$ cross section is estimated to be $\leq \pm 30\%$ which is in addition to the primarily statistical error of each cross section data point.

The results on the differential cross sections are shown in Fig. 2. The angular distributions of ${}^3\text{He}(\pi^-, \pi^0){}^3\text{H}$ are found to be featureless in the an-

gular range of $60^\circ \leq \theta \leq 135^\circ$ with a slight decrease in slope with increasing angle. These data cover the momentum transfer region $0.5 \leq q \leq 1.0 \text{ GeV}/c$. The invariant differential cross section $d\sigma/dt(q)$ (with $t = -2q^2$) is presented in Fig. 3 along with results at $T = 200, 250,$ and 295 MeV from the previous experiment⁴ and from another experiment¹⁰ at 131 and 142 MeV. From the data in Fig. 3 we infer an exponential q dependence of the (π^-, π^0) cross section but an additional energy dependent factor must be included for energies above 300 MeV. The ${}^3\text{He}(\pi^-, \pi^0){}^3\text{H}$ cross section at fixed scattering angle (Fig. 4) decreases continuously from 130 to 525 MeV by a factor of 200, which is due to a combination of the q and T dependencies.

Recently published Glauber calculations of Gerace *et al.*¹¹ represent the only attempt to predict ${}^3\text{He}(\pi^-, \pi^0){}^3\text{H}$ above 300 MeV. These calculations use π - N amplitudes obtained from $l=0$ and 1 phase shifts. The non-spin-flip and spin-flip π - N amplitudes are used in combination with ${}^3\text{He}$ form factors derived from electron scattering. Besides single scattering, multiple scattering and some higher order terms are included, but with spin-flip allowed only

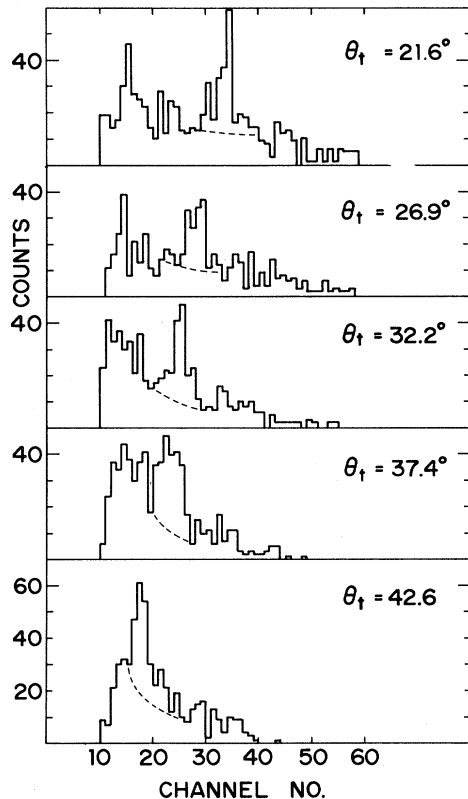


FIG. 1. Triton spectra for the reaction $\pi^- + {}^3\text{He} \rightarrow n + {}^3\text{H}$ at $T_\pi = 285 \text{ MeV}$ and a detector angle setting of $\theta_D = 32.5^\circ$. The abscissa is detector pulse height representing kinetic energy. The five spectra (from top to bottom) are for angular bins of about 5° centered at $\theta_L = 21.6, 26.9, 32.2, 37.4,$ and 42.6° . The peak is due to the (π^-, π^0) reaction and the dashed line indicates the estimated background.

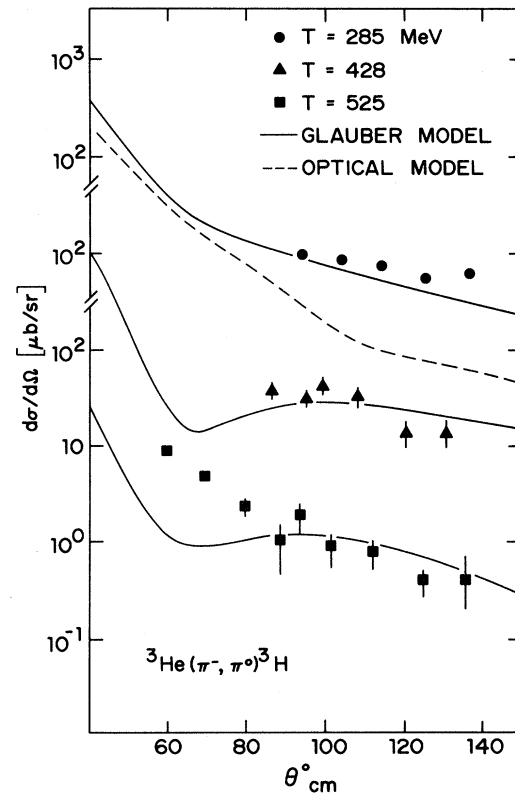


FIG. 2. Results on the differential cross sections of ${}^3\text{He}(\pi^-, \pi^0){}^3\text{H}$ at 285, 428, and 525 MeV. The solid curves are Glauber model calculations (Ref. 11) and the dashed curve is an optical model calculation (Ref. 3).

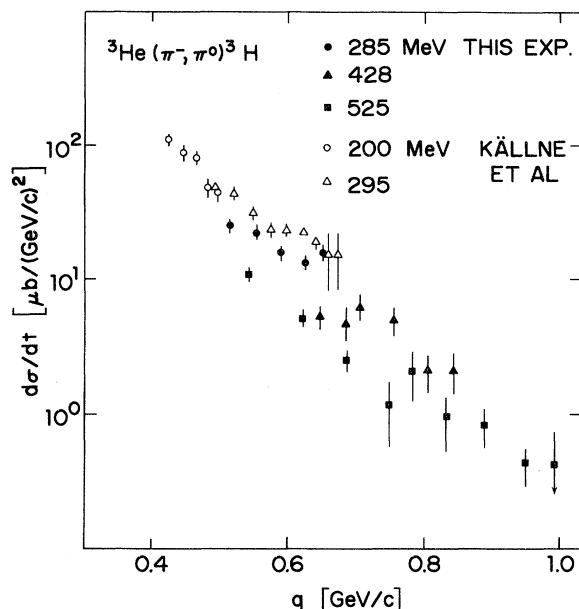


FIG. 3. The invariant differential cross section of ${}^3\text{He}(\pi^-, \pi^0){}^3\text{H}$ from the present and previous measurements (Ref. 4) plotted vs momentum transfer.

once. The results of these calculations are compared with our angular distributions in Fig. 2 and the predicted energy dependence of $d\sigma/d\Omega(\theta=120^\circ)$ is shown in Fig. 4 together with all available experimental results covering the energy range 130–525 MeV. Except for a region around 200 MeV agreement is fair. It is found by Gerace *et al.* that the bulk of the predicted cross section around $\theta=90^\circ$ is due to spin-flip contributions and is therefore sensitive to the ${}^3\text{He}$ magnetic form factor.

The magnetic form factor used in this calculation was obtained from a fit to electron scattering extending only up to $q \cong 700$ MeV/c. In the region up to 1 GeV/c, which is sampled by the pion SCE scattering at 525 MeV, the extrapolated form factor has a minimum at $q \approx 780$ MeV/c whereas according to new measurements it is at ~ 900 MeV/c. This minimum in the magnetic form factor is not apparent in the (π^-, π^0) cross section; this may indicate that it is filled in by contributions from the charge form factor, which has a maximum in the momentum range of the magnetic form factor minimum. Multiple scattering and other higher order terms are in principle also able to fill in minima but their contributions in the Glauber model are small. The relative weight of single scattering versus multiple scattering and other higher order terms might be a weak point of the Glauber model calculations because of the small angle scattering approximations upon which they rely. For single scattering there should be an equivalence between the Glauber model and the first order optical model.

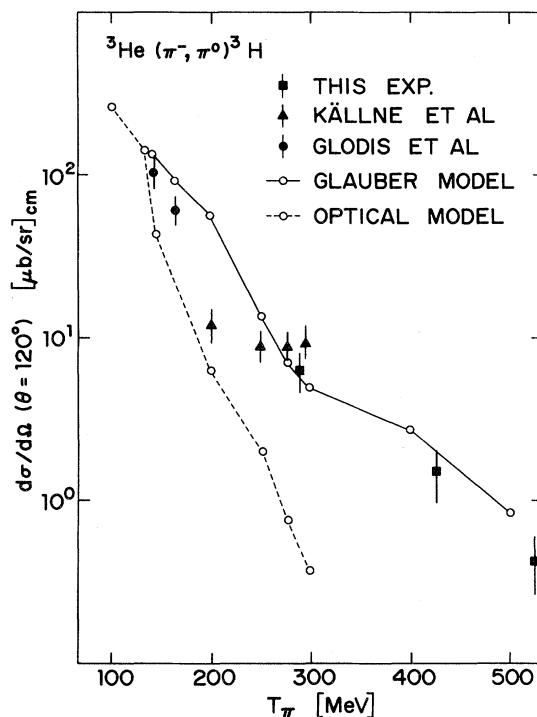


FIG. 4. The differential cross section of ${}^3\text{He}(\pi^-, \pi^0)$ at $\theta=120^\circ$ from this and previous (Refs. 4 and 10) experiments plotted vs incident energy. The solid and dashed curves are Glauber (Ref. 11) and optical (Ref. 3) model calculations.

First order optical model calculations have been performed³ by Landau and Wakamatsu for the ${}^3\text{He}(\pi^-, \pi^0){}^3\text{H}$ up to 295 MeV. The essential features of this calculation are (1) a first order, momentum space potential in a relativistic wave equation; (2) a πN amplitude $t_{\pi N}$ determined from πN phase shifts, including finite-size effects; and (3) realistic form factors. At 295 MeV the optical model predictions (Fig. 2) are lower than the Glauber result and underestimate the data by a factor of 5. Second order effects were specifically examined by Wakamatsu³ who found them to be small, at the level of $\leq 25\%$. The low cross section of the optical model at 295 MeV seems to be part of a trend where the gap between theory and experiment increases with increasing energy at least for energies above 200 MeV (Fig. 4); the results of Landau are shown in Fig. 4, which are similar to those of Wakamatsu in the region of overlap (200–295 MeV). It also appears that 200 MeV seems to be the energy limit above which the optical model ceases to account for the $\pi+{}^3\text{He}$ elastic scattering cross section in the intermediate angle region with which we are concerned here.¹² There are also some difficulties with a Glauber model interpretation of the elastic data at high energies. We find the agreement between the

Glauber model and our high energy SCE scattering data as an encouraging starting point for further theoretical efforts to verify the predominant single spin-flip scattering indicated by this model.

In summary, we have presented cross sections from the first measurement of ${}^3\text{He}(\pi^-, \pi^0){}^3\text{H}$ at energies of $T \geq 300$ MeV. These results confirm earlier data at 295 MeV showing that this cross section is much larger than predicted by optical model calculations. Our data at 285, 428, and 525 MeV can be reproduced by Glauber model calculations. This agreement suggests dominant single spin-flip scattering in the region of intermediate angles (correspond-

ing to $q \approx 0.5-1.0$ GeV/ c) and dependence upon the ${}^3\text{He}$ magnetic form factor. There are major discrepancies between seemingly equivalent scattering theories and between theories and experiments for $\pi + {}^3, {}^4\text{He}$ scattering. The successful application of the Glauber model to ${}^3\text{He}(\pi^-, \pi^0){}^3\text{H}$ to these data may indicate the correct approach for additional theoretical work.

We are grateful for Dr. W. Gerace and Dr. R. Landau for providing us with their calculations. This work was supported by the U.S. Department of Energy and the National Science Foundation.

*Present address: Harvard-Smithsonian Center for Astrophysics, Cambridge, Mass. 02138.

¹J. S. McCarthy, I. Sick, and R. R. Whitney, Phys. Rev. C **15**, 1396 (1977); H. Collard *et al.*, Phys. Rev. **138**, 57 (1965).

²J. Cavedon (private communication).

³R. Landau, Phys. Rev. C **15**, 2127 (1977); and LAMPF Workshop on Pion Single Charge Exchange, 1979 (unpublished), p. 150; and M. Wakamatsu, Nucl. Phys. **A340**, 289 (1980).

⁴J. Källne *et al.*, Phys. Rev. Lett. **42**, 159 (1979).

⁵J. Källne *et al.*, Phys. Rev. Lett. **45**, 517 (1980).

⁶J. M. Eisenberg and V. B. Mandelzweig, Phys. Lett. **53B**, 405 (1975).

⁷R. D. Verbeck and R. J. Macek, IEEE Trans. Nucl. Sci. **NS-22** (1975).

⁸L. Orphanos *et al.*, Phys. Rev. Lett. **46**, 1562 (1981); J. Källne *et al.*, *ibid.* **40**, 378 (1978); and J. Källne *et al.*, Phys. Rev. C **24**, 1103 (1981).

⁹P. I. Bussey *et al.*, Nucl. Phys. **B58**, 363 (1973); and P. M. Ogden *et al.*, Phys. Rev. **137**, 3145 (1965).

¹⁰P. Glodis *et al.*, Phys. Rev. Lett. **44**, 234 (1980).

¹¹W. J. Gerace, J. P. Mestre, J. F. Walker, and D. A. Sparrow, Phys. Rev. C **22**, 1197 (1980); and private communication; and J. P. Mestre, thesis (University of Massachusetts, 19xx) (unpublished).

¹²J. Källne *et al.*, Phys. Lett. **B103**, 13 (1981).